IOPscience iopscience.iop.org

Home Search Collections Journals About Contact us My IOPscience

Molecular frame Auger electron energy spectrum from N_2

This content has been downloaded from IOPscience. Please scroll down to see the full text.

2012 J. Phys. B: At. Mol. Opt. Phys. 45 055601

(http://iopscience.iop.org/0953-4075/45/5/055601)

View the table of contents for this issue, or go to the journal homepage for more

Download details:

IP Address: 130.207.141.218
This content was downloaded on 15/12/2016 at 23:19

Please note that terms and conditions apply.

You may also be interested in:

Molecular frame photoemission in dissociative ionization of H2 and D2 induced by high harmonic generation femtosecond XUV pulses
P Billaud, M Géléoc, Y J Picard et al.

Asymmetry in the molecular-frame photoelectron angular distribution for oxygen 1s photoemission from CO2
R R Lucchese, H Fukuzawa, X-J Liu et al.

Probing ultrafast electronic and molecular dynamics with free-electron lasers
L Fang, T Osipov, B F Murphy et al.

High resolution kinetic energy release spectra and angular distributions
S Voss, A S Alnaser, X-M Tong et al.

Structure and fragmentation dynamics of N2+2 ions
M Ahmad, P Lablanquie, F Penent et al.

A vibrationally resolved C 1s-1}Auger spectrum of CO2
R Püttner, V Sekushin, G Kaindl et al.

Probing the dynamics of dissociation of methane following core ionization using three-dimensional molecular frame photoelectron angular distributions
J B Williams, C S Trevisan, M S Schöffler et al.

Resonant Auger electron angular distributions of CO in the molecular frame
G Prümper, D Rolles, H Fukuzawa et al.

J. Phys. B: At. Mol. Opt. Phys. **45** (2012) 055601 (8pp) doi:10.1088/0953-4075/45/5/055601

Molecular frame Auger electron energy spectrum from N_2

J P Cryan[1,2], J M Glownia[1,3], J Andreasson[4], A Belkacem[5], N Berrah[6], C I Blaga[7], C Bostedt[8], J Bozek[8], N A Cherepkov[9,10], L F DiMauro[7], L Fang[6], O Gessner[5], M Gühr[1], J Hajdu[4], M P Hertlein[11], M Hoener[6,11], O Kornilov[5,16], J P Marangos[12], A M March[13], B K McFarland[1,3], H Merdji[1,14], M Messerschmidt[8], V S Petrović[1,2], C Raman[15], D Ray[13], D A Reis[1,3], S K Semenov[9], M Trigo[1], J L White[1,3], W White[8], L Young[13], P H Bucksbaum[1,2,3] and R N Coffee[1,8]

[1] The PULSE Institute for Ultrafast Energy Science, SLAC National Accelerator Laboratory, 2575 Sand Hill Road, Menlo Park, CA 94025, USA
[2] Department of Physics, Stanford University, Stanford, CA 94305, USA
[3] Department of Applied Physics, Stanford University, Stanford, CA 94305, USA
[4] Laboratory of Molecular Biophysics, Department of Cell and Molecular Biology, Uppsala University, Husargatan, SE-75124 Uppsala, Sweden
[5] Ultrafast X-ray Science Laboratory, Chemical Sciences Division, Lawrence Berkeley National Laboratory, Berkeley, CA 94720, USA
[6] Department of Physics, Western Michigan University, Kalamazoo, MI 49008, USA
[7] The Ohio State University, Department of Physics, Columbus, OH 43210, USA
[8] The Linac Coherent Light Source, SLAC National Accelerator Laboratory, Menlo Park, CA 94025, USA
[9] State University of Aerospace Instrumentation, 190000 St. Petersburg, Russia
[10] Institute fur Kernphysik, University Frankfurt, Max-von-Laue-Strasse 1, D-60438 Frankfurt, Germany
[11] Advanced Light Source, Lawrence Berkeley National Laboratory, Berkeley, CA 94720, USA
[12] Blackett Laboratory, Imperial College London, London SW7 2AZ, UK
[13] Argonne National Labortory, Argonne, IL 60439, USA
[14] CEA-Saclay, IRAMIS, Service des Photons, Atomes et Molecules, 91191 Gif-sur-Yvette, France
[15] School of Physics, Georgia Institute of Technology, Atlanta, GA 30332, USA

E-mail: jcryan@stanford.edu

Received 12 October 2011, in final form 2 January 2012
Published 14 February 2012
Online at stacks.iop.org/JPhysB/45/055601

Abstract
Here we present the first angle-resolved, non-resonant (normal) Auger spectra for impulsively aligned nitrogen molecules. We have measured the angular pattern of Auger electron emission following *K*-shell photoionization by 1.1 keV photons from the Linac Coherent Light Source (LCLS). Using strong-field-induced molecular alignment to make molecular frame measurements is equally effective for both repulsive and quasi-bound final states. The capability to resolve Auger emission angular distributions in the molecular frame of reference provides a new tool for spectral assignments in congested Auger electron spectra that takes advantage of the symmetries of the final diction states. Based on our experimental results and theoretical predictions, we propose the assignment of the spectral features in the Auger electron spectrum.

(Some figures may appear in colour only in the online journal)

[16] Present address: Max Born Institute, Berlin, Germany.

 © 2012 IOP Publishing Ltd Printed in the UK & the USA

1. Introduction

In molecules with low-Z atomic constituents, photo-ionization of a K-shell electron is predominantly followed by rapid KLL-Auger electron emission. The result of this two-step process is an excited molecular dication with two vacancies in the valence or inner valence shells. While non-resonant Auger electron emission from molecules is typically isotropic in the laboratory frame [1–3], in the molecular frame of reference, anisotropic Auger electron distributions are observed that reflect (i) the angular symmetries of the wavefunctions involved in the decay process, (ii) two-centre interference effects and (iii) scattering of the outgoing Auger electron by the molecular potential [4–7]. The emission angle in the molecular frame is particularly interesting because it shows how the electron correlation interaction that gives rise to the Auger decay process is influenced by the molecular structure. In this paper, the correlation between final state symmetries and molecular frame Auger angular distributions supports a revision of previous spectral assignments of several Auger lines in the highly congested region of the normal KLL-Auger spectrum of N_2.

The nitrogen dication is generally unstable and undergoes spontaneous dissociation. Depending on its state of excitation, it may rapidly separate into fragment ions via steep ionic potential energy surfaces. In such cases, measuring the angle of the dissociating fragments provides the crucial missing information about the molecule's orientation during the Auger electron emission. In many cases, however, the molecule is quasi-bound and requires time to tunnel through a potential energy barrier in order to dissociate. The molecule's rotation then destroys this connection between the fragment angle and the molecular orientation during Auger emission.

In this paper, we present a novel approach to angle-resolved Auger electron spectroscopy (ARAES) that provides molecular frame information. We observe the ARAES for numerous KLL-transitions in diatomic nitrogen, N_2, with electron energies in the range of 357–370 eV. Figure 1 shows the molecular potential energy curves for the N_2^{2+} final states considered in this work. We see that in addition to the dissociative final states, there are a number of quasi-bound final states that are inaccessible to traditional coincidence-based ARAES techniques [5–14].

In traditional ARAES, electrons are collected in coincidence with fragment ions. Either fragment ions are collected in coincidence with Auger electrons [5–9] or the fragment ions are collected in coincidence with photoelectrons [10–12]. In the latter case, the resulting Auger electron angular distribution is inferred from momentum conservation. In either case, the axis of fragmentation is assumed to reflect the original orientation of the parent molecule. This assumption is only true if dissociation is much faster than the typical timescale of rotation; a condition known as the axial recoil approximation [15, 16]. The rotational timescales for small, low-Z, molecules are typically on the hundreds of femtoseconds scale at room temperature and picoseconds scale in a supersonically cooled gas jet. If rotational motion occurs on a time scale that competes with dissociation, the axial recoil approximation

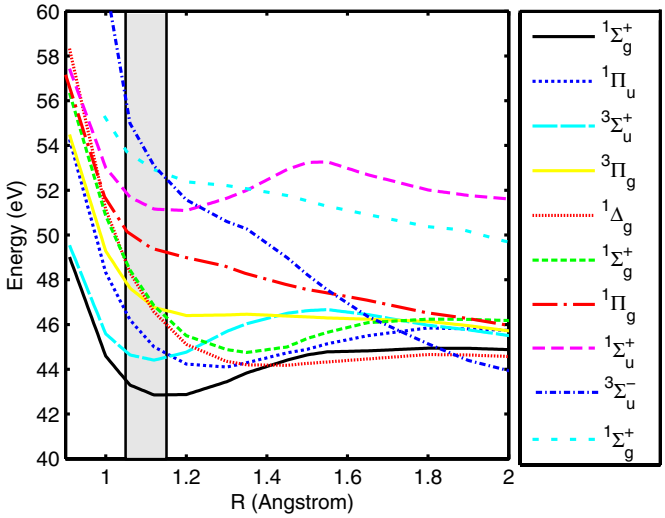

Figure 1. N_2^{2+} molecular potential energy surfaces from [17]. The energy is with respect to the v-0 energy of the $X^1\Sigma_g$ of N_2 [17]. The shaded area represents the Frank–Condon overlap with the ground state of N_2.

fails. This is exactly the case for quasi-bound final states of, e.g., N_2^{2+}, CO^{2+}, CO_2^{2+}, O_2^{2+} and $C_2H_2^{2+}$. Therefore, a technique that does not rely on the axial-recoil approximation is highly desirable. The technique presented in this work is equally effective for bound or dissociative final states.

The use of strong-field-induced molecular alignment [18] is common in optical laser-based molecular-frame photoelectron angular distribution (MF-PAD) experiments [19–21]. In this work, we use impulsive stimulated Raman scattering to transiently align the molecular axis of N_2 molecules with respect to the laboratory frame. Such non-resonant impulsive molecular alignment creates a rotational wave packet that exhibits field-free alignment revivals [18]. For N_2, these revivals have a window of some ∼200 fs within which the ensemble of molecules is aligned with respect to the laboratory frame. These periodic revivals repeat every 8.34 ps after the initial pulse.

Synchronization of the few-femtosecond x-ray pulses from the Linac Coherent Light Source (LCLS) to the transient alignment revival of an ensemble of N_2 molecules effectively leads to a photoionization experiment on molecules that are aligned in the laboratory frame in a field-free environment. This is essential to our study since the Auger decay process is extremely sensitive to external fields [22]. Spectroscopic studies on transiently aligned molecules were recently performed at two x-ray free electron laser facilities: the Free Electron Laser at Hamburg (FLASH) [23] and the LCLS [24, 25].

Here, we demonstrate how spectrally resolved molecular Auger electron angular emission patterns can be employed to incorporate molecular frame symmetries into the assignment of spectroscopic features. The angular distribution of Auger electrons resulting in the well-separated energy features near 366.8 eV, 360.3 eV, 359 eV and 357.4 eV can be measured by direct peak integration, without employing a nonlinear fitting procedure, as was done in [5]. These features are believed

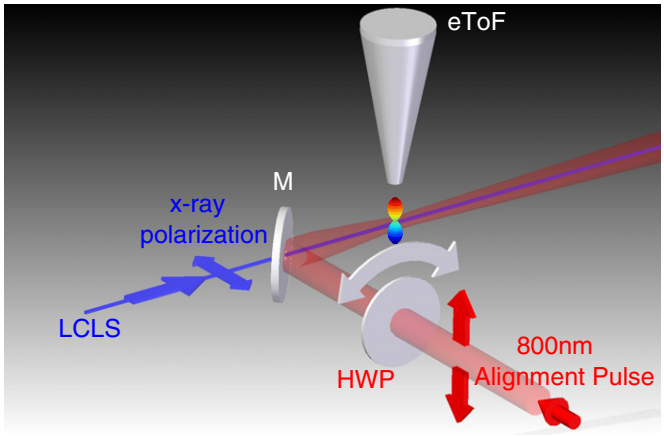

Figure 2. Experimental setup: electron time-of-flight (eTOF) spectrometer [31] is oriented perpendicular to the plane containing the x-ray polarization and propagation direction. X-rays co-propagate through the interaction region along with the 800 nm molecular alignment pulse. The axis of molecular alignment is controlled with a half-wave plate (HWP). Reproduced with permission from [24]. Copyright 2010 by The American Physical Society.

to result from transitions to the states: $X\,^1\Sigma_g^+$, $^1\Pi_g$, $^1\Sigma_u^+$ and $(2\sigma_u)^{-2}\ ^1\Sigma_g^+$, respectively, and these agree well with our angular calculations. Unlike reference [5], however, this work is able to measure Auger features which result in quasi-bound final dication states, the reference [5] technique was blind to the feature at 366.8 eV and some of the features at 359 eV. The states falling between 361 and 366 eV ($^3\Sigma_u^+$, $^1\Pi_u$, $^3\Pi_g$, $(1\pi_u)^{-2}\ ^1\Sigma_g^+$ and $^1\Delta_g$) heavily overlap, impeding spectral assignments. By including the angular information in a nonlinear fitting routine, we are able to make definitive assignments of these spectrally ambiguous Auger channels that contradict previous assignments [26–30].

2. Experiment

2.1. Experimental setup

We used linearly polarized 800 nm pulses with ∼60 fs square temporal profiles and ∼400 μJ pulse energies to align a ∼20 K N_2 target gas. The ∼20 K molecular beam was produced by a 100 μm diameter pulsed gas jet [32], and then passed through a 500 μm skimmer before entering the interaction region, where the 800 nm laser was focused to a spot size of ∼75 μm. The cold molecular ensemble transiently aligns along the direction of linear polarization of the 800 nm pulses [18]. We changed the direction of the alignment axis with respect to the laboratory frame by rotating the polarization of the laser pulse with a HWP. Our experimentally derived degree of alignment, published elsewhere [25], was estimated to be $\langle\cos^2\theta\rangle_{\max} \sim 0.65$.

The LCLS produced 1.1 keV x-ray pulses shorter than 5 fs, containing $\sim 10^{12}$ photons ($\sim 2\times 10^{11}$ photons after transport). The accelerator was operated in low bunch charge (20 pC) mode, keeping the electron bunch very near full longitudinal compression to produce such short pulses. A Kirkpatrick–Baez mirror pair focussed the 25 μJ x-ray beam to a spot size of ∼3 μm through a 2 mm hole in the mirror that combines the x-rays and 800 nm pulses as shown in figure 2. The relative timing between the IR and x-ray laser pulses was maintained to better than ∼100 fs using the technique described in [25]. Further details of the experimental setup are given in [24, 25].

Electrons were collected with a retarding field electron time-of-flight (eTOF) spectrometer oriented as shown in figure 2. This spectrometer was operated in the single count regime with a count rate of ∼0.016 counts/shot. To increase the energy resolution of the spectrometer, the retarding lens, detailed in [31], was operated with a 350 V retardation giving an energy resolution between 60 and 200 meV in the region of the spectrum between 350 and 370 eV. The Auger emission pattern was mapped out by rotating the polarization of the molecular alignment laser in three different orientations of the molecular axis relative to the detector axis: 0°, 45° and 90°. The Auger electron spectrum (AES) for each orientation is shown in figure 3 and each spectrum has been corrected for the energy-dependent transmission efficiency of the spectrometer which was calculated using SIMION [33]. The corresponding yield for a given molecular orientation is a convolution of the angle dependence of the Auger decay process with the angle dependence of the photoionization process. For photon energies $\geqslant$100 eV above the characteristic absorption edge, the photoionization process is insensitive to the orientation between the x-ray polarization and the molecular axis [34, 35]. So at ∼700 eV above the N_2 K-edge, the photoionization cross-section is identical for all three orientations investigated; any anisotropy observed in the Auger

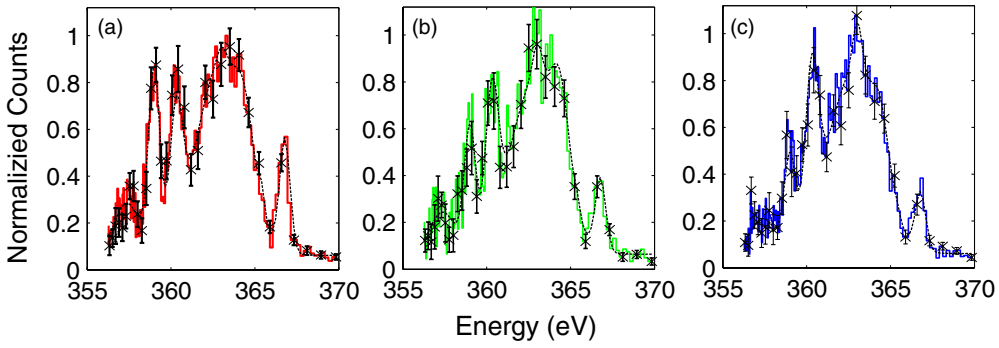

Figure 3. Auger electron spectra of N_2 molecules at emission angles of (a) 0°, (b) 45° and (c) 90° relative to the molecular axis. Spectra are shown with representative error bars and the minimum χ^2 fit to the data.

electron yield is due to the angular dependence of the Auger decay process itself.

2.2. Nonlinear fitting

Many states contribute to the rich AES of molecular nitrogen. We use a nonlinear optimization procedure to identify the contribution for individual spectral features. Our optimization routine minimizes the quantity

$$\chi^2 = \sum_{\theta=0^\circ,45^\circ,90^\circ} \left[\sum_E \left(\frac{S(E,\theta) - f(E,\theta)}{\sigma(E,\theta)} \right)^2 + \sum_{i=1}^{9} \left(\frac{A_i Y_i(\theta) - y_i(\theta)}{A_i \Delta_i(\theta)} \right)^2 \right], \quad (1)$$

where $S(E,\theta) \pm \sigma(E,\theta)$ is the measured AES and associated error at energy E and angle θ to the molecular axis. $Y_i(\theta) \pm \Delta_i(\theta)$ is the calculated yield of Auger electrons at an angle θ to the molecular axis, resulting from the ith final state ($i = X\,^1\Sigma_g^+$, $^3\Sigma_u^+$, $^1\Pi_u$, $^3\Pi_g$, $(1\pi_u)^{-2}\,{}^1\Sigma_g^+$, $^1\Delta_g$, $^1\Pi_g$, $^1\Sigma_u^+$ and $(2\sigma_u)^{-2}\,{}^1\Sigma_g^+$). The fit to the signal, $f(E,\theta)$, and the total electron yield for a given final state, $y_i(\theta)$, are defined as

$$f(E,\theta) = o(\theta) + \sum_{i=1}^{9} a_i(\theta) \mathrm{Exp}\left(-\left[\frac{E - b_i}{c_i} \right]^2 \right) \quad (2)$$

$$y_i(\theta) = a_i(\theta) c_i, \quad (3)$$

where $a_i(\theta)$, b_i, c_i and $o(\theta)$ are fitting paramters, and A_i is a scaling factor between the yield from fit and the calculation.

The optimization routine used a Nelder–Mead simplex algorithm [36], which is employed in the MATLAB [37] *fminsearch*( ) function. The routine is seeded with central energies, line widths and peak amplitudes that are consistent both with a rough qualitative estimate and with the results reported in [26] and [28]. The fit result was determined to be the global minimum based on Monte Carlo-based sampling of the seed parameter space.

The calculated Auger electron angular distributions used in the fitting procedure are described in detail in [12, 38] and shown in figure 4. Also shown are convolutions of the calculated Auger electron angular distributions with our previously measured molecular alignment distribution. This ensemble alignment is measured by fitting the transient signal of ion fragmentation versus delay between the aligning laser pulse and the x-rays as described in [25]. For the purpose of fitting, we assume a 10% error for the calculated distributions, i.e. $\Delta_i(\theta) \sim 0.1 Y_i(\theta)$.

3. Results and discussion

The results of our nonlinear fitting routine are shown in figures 3, 5 and 6 and the parameters are compiled in table 1. We find that including the angular information significantly restricts the results of the nonlinear fitting algorithm. Including this added information allows us to make a more definitive assignment of the features in the Auger electron energy

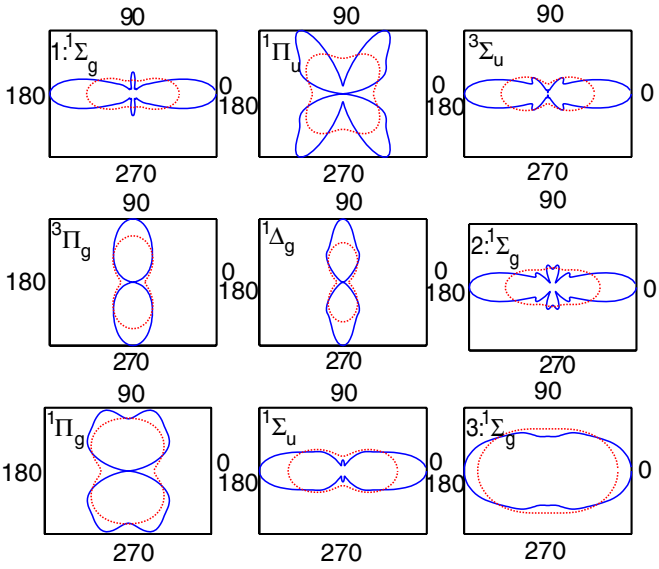

Figure 4. Theoretical Auger electron angular distributions for the final dicationic states studied in this work. The molecular axis lies along the horizontal. The solid curve shows the calculation while the dashed curve shows the calculation convolved with our molecular ensemble distribution. The $^1\Sigma_g$ states are labelled as follows: (1) $(3\sigma_g)^{-2}$ X-state, (2) $(1\pi_u)^{-2}$, (3) $(2\sigma_u)^{-2}$.

spectrum for both dissociative and quasi-bound final states of the nitrogen dication. Consistent with previous findings, we observe the yield of triplet final states to be very low compared to the yield from singlet states. It is worth noting that the fit results for the $^1\Pi_g$ have the worst agreement in the angular yield (figure 6) of any of the Auger electron energy features, but the recovered angular yield is consistent with recent measurements made using a coincidence technique [5]. This difference between the calculated and measured yield is not well understood at this point. The most striking difference, however, lies in the energy ordering of states. Our fitting routine finds that the $(1\pi_u)^{-2}$: $^1\Sigma_g^+$ and $^1\Delta_g$ states are interchanged with respect to previous energy assignments (see table 1). Our analysis also finds that the $^3\Sigma_u^+$ and $^1\Pi_u$ ordering is interchanged relative to previous identifications.

There is large uncertainty in the assignment of different peaks in the N_2 *KLL* AES. In the region of the spectrum between 361 and 366 eV, the measured energies of the Auger lines vary widely between different experiments and calculations [26–30]. Calculated energies are known to have predictive errors in the order of the energy difference between the different electronic states [12, 38]. Given the difficulty in accurately predicting the molecular AES, it is no surprise that there is some disagreement in the energy assignments, as shown in table 1.

Previous spectroscopic assignments were based on calculations of the Auger electron energy, width and relative yields. Frank–Condon (FC) arguments have allowed feature widths to aid the line identifications in recent articles as well as in this work [12, 38]. In figure 1, we show some representative final dicationic states for N_2 along with the shaded representation of the FC region. The FC region is bounded by the inner and outer classical turning points of the

Table 1. N_2 *KLL* Auger transition energies from our nonlinear fit shown in figure 3. Our results are shown in the right-most part of the table, and the result from several other previous studies are shown for comparison. The errors in the fit parameters have been estimated following the method described in [39].

	Reference [27][a]		Reference [26][b]			Reference [28]	Our Results					Yield		
Final Electronic	Eng.	Yield	Eng.	FWHM	Yield	Energy (eV)	Energy (eV)			FWHM		Exp.		Calc.
State of N_2^{2+}	(eV)	(%)	(eV)	(eV)	(%)	Rel. (Abs.)	Rel.	(Abs.)	±	eV	(±)	%	(±)	%
$(3\sigma_g)^{-2}\ X^1\Sigma_g^+$	0.0	8.8	0.21	0.5	2.2	0.00 (366.90)	0.00	(366.79)	0.03	0.73	(0.04)	5.4	(0.5)	20.8
$(3\sigma_g)^{-1}(2\sigma_u)^{-1}\ ^3\Sigma_u^+$	1.56	3.8	2.8	1.92	34	1.81 (365.09)	1.4	(365.4)	0.2	0.4	(0.1)	1	(4)	4.35
$(3\sigma_g)^{-1}(1\pi_u)^{-1}\ ^1\Pi_u$	1.24	14	1.4	1.4	5.2	1.58 (365.32)	2.39	(364.40)	0.07	1.3	(0.2)	7	(1)	11.4
$(2\sigma_u)^{-1}(1\pi_u)^{-1}\ ^3\Pi_g$	2.55	1	3.9	0.95	11	2.81 (364.09)	3.8	(363.0)	0.1	0.7	(0.2)	2	(2)	2.15
$(1\pi_u)^{-2}\ ^1\Sigma_g^+$	3.39	14	5.3	1.1	10	4.00 (362.90)	3.8	(363.0)	0.1	3.3	(0.2)	38	(1)	10.5
$(1\pi_u)^{-2}\ ^1\Delta_g$	3.27	24	4.6	0.79	7.3	2.78 (364.12)	4.3	(362.5)	0.1	3.7	(0.2)	19	(1)	8.01
$(2\sigma_u)^{-1}(1\pi_u)^{-1}\ ^1\Pi_g$	5.54	9.8	6.3	0.84	14	6.47 (360.40)	6.47	(360.31)	0.04	0.89	(0.05)	11	(1)	7.79
$(3\sigma_g)^{-1}(2\sigma_u)^{-1}\ ^1\Sigma_u^+$	6.86	17	7.7	0.57	9.6	7.73 (359.07)	7.79	(359.00)	0.04	0.80	(0.04)	9.4	(0.4)	21.6
$(2\sigma_u)^{-2}\ ^1\Sigma_g^+$	9.59	7.6	9.3	1.8	6.7	9.83 (357.07)	9.4	(357.4)	0.2	1.8	(0.2)	7.0	(0.6)	13.6

[a] Energy relative to 370.33 eV.

[b] Energy relative to 366.9 eV.

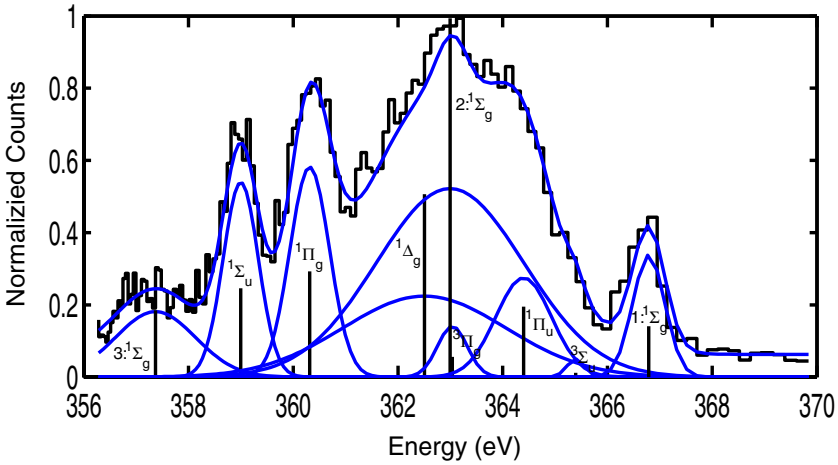

Figure 5. N_2 AES for unaligned ensemble of molecules. The curves below the composite spectrum indicate each feature's contribution to the total spectrum and are labelled next to the peak. The $^1\Sigma_g$ states are labelled as follows: (1) $(3\sigma_g)^{-2}$ X-state, (2) $(1\pi_u)^{-2}$, (3) $(2\sigma_u)^{-2}$.

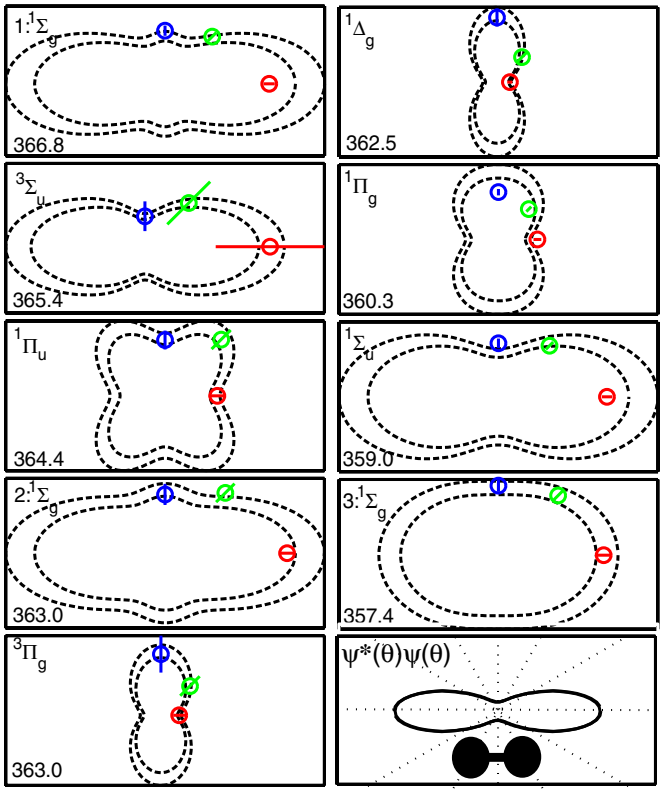

Figure 6. The yield of Auger electrons as a function of angle from our theory-guided nonlinear fit (circles) and associated uncertainty (bars). The molecular axis is aligned along the horizontal axis. The dashed curve (black) represents the ±10% error of our calculation from figure 4 convolved with our measured molecular ensemble distribution. Each panel is labelled by the central energy of the Auger feature (bottom-left corner) and the assigned final state (upper-left corner). The $^1\Sigma_g$ states are labelled as follows: (1) $(3\sigma_g)^{-2}$ X-state, (2) $(1\pi_u)^{-2}$, (3) $(2\sigma_u)^{-2}$. The bottom-right panel shows the predicted molecular distribution $(\psi^*(\theta)\psi(\theta))$ from the data in [25].

neutral ground-state potential surface. Looking qualitatively at these curves, an Auger transition that results in the quasi-bound $X\,^1\Sigma_g^+$ state would resemble a narrow atomic Auger transition, while transitions leading to final configurations of $(1\pi_u)^{-2}$, either the $^1\Delta_g$ or $^1\Sigma_g^+$ highly dissociative final dication states would be very broad in Auger electron energy. In fact, these two particular dissociative states are very similar in energy, width and amplitude (see figure 5), yet according to figure 4 they exhibit very distinct angular Auger emission patterns. Our assignment is based on the angular yield information shown in figure 6; the feature at 363 eV has the greatest yield along the molecular axis (consistent with the $^1\Sigma_g^+$ state), whereas the feature at 362.5 eV has its highest yield orthogonal to the axis (consistent with the $^1\Delta_g$ state). The addition of angular information points to a reversal of previous identifications [26–28] for these two $(1\pi_u)^{-2}$ configurations.

In diatomic nitrogen, the assignment of spectral features to quasi-bound final states is unambiguous, but the corresponding angular distributions of Auger electrons have never been measured. The quasi-bound states determined from figure 1 are the $X\,^1\Sigma_g^+$, the $^1\Sigma_u^+$ and the $^3\Sigma_u^-$ states. High-resolution electron spectroscopy has resolved vibrational structure for the first two quasi-bound states mentioned [28, 40]. Although we do not resolve the individual vibrational peaks, we nevertheless measure for the first time the angular distribution of Auger electrons resulting from these transitions. We find that these Auger features associated with decay to these quasi-bound final states show good agreement with our calculated angular yields.

4. Conclusion

We have found that the angular dependence of the Auger electron energy spectrum provides useful added information for assigning spectral features to particular molecular Auger decay processes. Previously, channel assignments were based on energy calculations which led to numerous inconsistencies even for the intensely studied N_2 molecule [26–30]. More recent identifications included relative yields and relative widths in addition to the energy calculations [11, 12]. The angular patterns of Auger electrons from different decay

channels are markedly different as shown in figure 4 and provide better insight into the specific electronic states involved in the process. As an example from this work, the measured angular distributions allow identification of the two terms of the $(1\pi_u)^{-2}$ configuration which otherwise overlap substantially in the spectrum. Future higher angular resolution work is being planned for both non-resonant and near-resonant x-ray absorption that would resolve some of the finer details of calculated angular patterns.

Quasi-bound final states resulting from Auger relaxation have dissociation times orders of magnitude longer than the rotational period of a molecule. This voids the application of axial-recoil-based methods to measure molecular frame Auger electron angular distributions. Then, the only way to study these states is by knowing the molecular orientation *a priori*. Adiabatic molecular alignment is a common technique for obtaining very high degrees of molecular alignment in the laboratory frame [21]. Unfortunately the alignment only exists while a strong laser field is applied, mixing the valence electronic states and breaking the natural molecular symmetries. By using impulsive molecular alignment, we photoionized the molecular ensemble only during a period of full quantum revival of the ensemble alignment. Working at the recurrence of the alignment signal, we measured the photoionization-Auger decay process, in the molecular frame, in the absence of an external field.

Our technique reveals the molecular-frame angular distributions of Auger electron emission for both quasi-bound and dissociative final dication states while preserving reasonably high energy resolution. High energy resolution ARAES spectroscopy could be of great interest for future time-resolved molecular dynamics investigations. Time-resolved photo-chemistry could be probed by the transient shifting of Auger energy peaks as a molecule proceeds through a reaction. The transient shifts will likely be of the order of hundreds of meV, requiring the high energy resolution. The reactions are also likely to change the electronic symmetry of the reacting molecule as it isomerizes or a functional group dissociates, necessarily violating the axial recoil approximation. Such changes in electronic symmetry could be probed via angular electron emission patterns such as ARAES. The technique presented here can run with higher ($\sim \times 10$) event rates than in the current work to compensate the typically low collection efficiency of high-resolution electron spectrometers. It is perhaps the most viable way to collect ARAES with high energy resolution, free of strong laser fields and immune to the necessarily broken axial-recoil approximation.

Acknowledgments

Portions of this research were carried out at the Linac Coherent Light Source (LCLS) at the SLAC National Accelerator Laboratory. LCLS is an Office of Science User Facility operated for the US Department of Energy Office of Science by Stanford University. The authors would like to thank Christian Buth for useful discussions regarding this manuscript, Rick Iverson, Paul Emma, Zhirong Huang and Yuantao Ding for their unwavering pursuit of sub-10 fs xFEL pulses, and Bertold Krässig for his work modelling the eTOF spectrometers. This research is supported through both the LCLS at the SLAC National Accelerator Laboratory and the Chemical Science Division of the US Department of Energy, Office of Basic Energy Sciences, Chemical, Geosciences, and Biological Divisions. AB, OG and OK were supported by the Director, Office of Science, Office of Basic Energy Sciences, Chemical Sciences Division of the US Department of Energy under contract no DE-AC02-05CH11231. CIB and LFD acknowledge support from the NSF grant PHY-1004778.

References

[1] Lindle D W, Truesdale C M, Kobrin P H, Ferrett T A, Heimann P A, Becker U, Kerkhoff H G and Shirley D A 1984 *J. Chem. Phys.* **81** 5375
[2] Becker U, Hölzel R, Kerkhoff H G, Langer B, Szostak D and Wehlitz R 1986 *Phys. Rev. Lett.* **56** 1455
[3] Truesdale C M, Lindle D W, Kobrin P H, Becker U E, Kerkhoff H G, Heimann P A, Ferrett T A and Shirley D A 1984 *J. Chem. Phys.* **80** 2319
[4] Sann H *et al* 2011 *Phys. Rev. Lett.* **106** 133001
[5] Rolles D, Prümper G, Fukuzawa H, Liu X-J, Harries J, Ueda K, Pesic Z D, Dumitriu I and Berrah N 2010 *J. Phys.: Conf. Ser.* **212** 012009
[6] Prümper G, Fukuzawa H, Rolles D, Sakai K, Prince K C, Harries J R, Tamenori Y, Berrah N and Ueda K 2008 *Phys. Rev. Lett.* **101** 233202
[7] Prümper G, Rolles D, Fukuzawa H, Liu X J, Pešić Z, Dumitriu I, Lucchese R R, Ueda K and Berrah N 2008 *J. Phys. B: At. Mol. Opt. Phys.* **41** 215101
[8] Edwards A K, Zheng Q, Wood R M and Mangan M A 1997 *Phys. Rev.* A **55** 4269
[9] Zheng Q, Edwards A K, Wood R M and Mangan M A 1995 *Phys. Rev.* A **52** 3940
[10] Schöffler M S *et al* 2008 *Science* **320** 920
[11] Cherepkov N A *et al* 2009 *Phys. Rev.* A **80** 051404
[12] Semenov S K *et al* 2010 *Phys. Rev.* A **81** 043426
[13] Rolles D, Prümper G, Fukuzawa H, Liu X-J, Pesic Z D, Fink R, Grum-Grzhimailo A N, Dumitriu I, Berrah N and Ueda K 2008 *Phys. Rev. Lett.* **101** 263002
[14] Ulrich J, Moshammer R, Dorn A, Dörner R, Schmidt L P H and Schmidt-Böcking H 2003 *Rep. Prog. Phys.* **66** 1463
[15] Zare R N 1967 *J. Chem. Phys.* **47** 204
[16] Wood R M, Zheng Q, Edwards A K and Mangan M A 1997 *Rev. Sci. Instrum.* **68** 1382
[17] Wetmore R W and Boyd R K 1986 *J. Phys. Chem.* **90** 5540
[18] Stapelfeldt H and Seideman T 2003 *Rev. Mod. Phys.* **75** 543
[19] Bisgaard C Z, Clarkin O J, Wu G, Lee A M D, Gessner O, Hayden C C and Stolow A 2009 *Science* **323** 1464
[20] Kumarappan V, Holmegaard L, Martiny C, Madsen C B, Kjeldsen T K, Viftrup S S, Madsen L B and Stapelfeldt H 2008 *Phys. Rev. Lett.* **100** 093006
[21] Holmegaard L *et al* 2010 *Nature Phys.* **6** 428
[22] Buth C and Schafer K J 2009 *Phys. Rev.* A **80** 033410
[23] Johnsson P *et al* 2009 *J. Phys. B: At. Mol. Opt. Phys.* **42** 134017
[24] Cryan J P *et al* 2010 *Phys. Rev. Lett.* **105** 083004
[25] Glownia J M *et al* 2010 *Opt. Express* **18** 17620
[26] Víkor G, Ricz S, Tóth L, Sulik B, Végh J, Kövér A and Kövér L 1997 *Nucl. Instrum. Methods Phys. Res.* B **124** 393
[27] Ågren H 1981 *J. Chem. Phys.* **75** 1267
[28] Sorensen S L, Miron C, Feifel R, Piancastelli M-N, Björenholm O and Svensson S 2008 *Chem. Phys. Lett.* **456** 1

[29] Svensson S, de Brito A N, Keane M P, Correia N, Karlsson L, Liegener C-M and Ågren H 1992 *J. Phys. B: At. Mol. Opt. Phys.* **25** 135
[30] Moddeman W E, Carlson T A, Krause M O and Pullen B P 1971 *J. Chem. Phys.* **55** 2317
[31] Hemmers O, Whitfield S B, Glans P, Wang H, Lindle D W, Wehlitz R and Sellin I A 1998 *Rev. Sci. Instrum.* **69** 3809
[32] Proch D and Trickl T 1989 *Rev. Sci. Instrum.* **60** 713
[33] Dahl D A 2010 *SIMION 3D Version 8.0* (Idaho: Idaho National Engineering and Environmental Laboratory)
[34] Kivimäki A, Neeb M, Kempgens B, Köppe H M and Bradshaw A M 1996 *Phys. Rev.* A **54** 2137
[35] Dill D, Swanson J R, Wallace S and Dehmer J L 1980 *Phys. Rev. Lett.* **46** 1393
[36] Lagarias J C, Reeds J A, Wright M H and Wright P E 1998 *SIAM J. Optim.* **9** 112
[37] MATLAB 2009 *version 7.9.0.529 (R2009b)* (Natick, MA: The MathWorks Inc.)
[38] Semenov S K, Kuznetsov V V, Cherepkov N A, Bolognesi P, Feyer V, Lahmam-Bennani A, Casagrande M E S and Avaldi L 2007 *Phys. Rev.* A **75** 032707
[39] Cumpson P J and Seah M P 1992 *Surf. Interface Anal.* **18** 345
[40] Püttner R, Fukuzawa H, Liu X-J, Semenov S K, Cherepkov N A, Tanaka T, Hoshino M, Tanaka H and Ueda K 2008 *J. Phys. B: At. Mol. Opt. Phys.* **41** 141001